International Journal of
Advanced Thermofluid Research

ISSN 2455-1368
www.ijatr.org

Thermal Radiation on Transient Laminar Gray Gas Flow Past an Oscillating Vertical Plate with Variable Temperature

Swapan Kumar Ghosh [1*], Sanatan Das [2], Rabindra Nath Jana [3] and Ayan Ghosh [4]

[1]*Department of Mathematics, Narajole Raj College, Narajole 721211, West Bengal, India.*
[2]*Department of Mathematics, University of Gour Bnaga, Malda 732 103, West Bengal, India.*
[3]*Department of Applied Mathematics, Vidyasagar University, Midnapore 721 102, West Bengal, India.*
[4]*Department of Mechanical Engineering, Seacom Engineering College, Howrah 711 302, West Bengal, India.*

Keywords
Thermal Radiation •
Gray Gas Flow •
Grashof Number •
Rosseland Model •
Radiative Heat-flux.

Abstract

Authors have presented an analytical approach on transient laminar gray gas flow past an oscillating vertical flat plate in the presence of natural convection and radiation. The fluid is considered to be a gray, absorbing-emitting radiation but non- scattering medium. The Rosseland flux approximation is employed to simulate radiation heat transfer contribution. We have also studied Stoke's first and second problem to justify the physical significance on this problem. This problem is solved by employing Laplace Transform method. Numerical results of velocity and temperature distributions are depicted graphically. Also, numerical results of frictional shearing stress and critical Grashof number are presented in tables.

Received Oct 18, 2015 **Revised** Nov 21, 2015 **Accepted** Nov 28, 2015 **Published** Dec 01, 2015

***Corresponding email**: g_swapan2002@yahoo.com (Swapan KumarGhosh).

DOI: https://doi.org/10.51141//IJATR.2015.1.2.1

Nomenclature

g	Gravity acceleration
$\mathrm{Gr}\left(=\frac{g\beta\nu(T'_w - T'_\infty)}{u_0^3}\right)$	Grashof number
$i\left(=\sqrt{-1}\right)$	Complex unity
k	Thermal conductivity
k^*	Rosseland mean absorption coefficient
$\mathrm{k}_1\left(=\frac{16\sigma T'^3_\infty}{3kk^*}\right)$	Radiation parameter

$\Pr\left(=\frac{\nu}{\alpha}\right)$	Prandtl number
q_r	The radiative heat flux
t'	Time
t	Non-dimensional time
T'	Fluid temperature
T'_w	Plate temperature
T'_∞	Ambient cold fluid
T	Non-dimensional fluid temperature
u_0	Characteristic velocity
u'	Fluid velocity
u	Non-dimensional fluid velocity
x', y'	Co-ordinate axes
y	Non-dimensional distance

Greek symbols

β	Thermal expansion coefficient
ν	Kinematic coefficient of viscosity
σ	Stefan-Boltzman constant
ρ	Density
ω'	Frequency of oscillations
$\omega\left(=\frac{\omega'\nu}{u_0^2}\right)$	Non-dimensional frequency of oscillations
ωt	Phase angle
τ_x	Shear stress

Subscripts

w	Plate surface
∞	Away from the plate

1. Introduction

The foundation of space laboratory was established by the concept of gray body radiation of its optical measurement. As the radiation from the external source passes through the medium from its boundary to a given point, it diminishes gradually at the expense of absorption. The radiation method is based on comparing the quantity of heat radiated by the solid investigated with that of a black body or another solid (standard), whose radiation factor or emissivity is known. A medium can be considered as some continuum of photons. Just as with molecular conductivity the transfer of radiant energy in a medium can be compared with diffusion transfer. Here the effect of interphoton collision is predominant. In this situation, Stefan-Boltzmann's law is strictly valid for a gray body to the same extent as the assumption that emissivity remains strictly constant,

independent of temperature. However, the emissivity of a gray body depends on its nature, temperature, state of the emitting surface and is usually determined by experiment. The study of transient laminar convection in the presence of thermal radiation attracts wide attention to many researchers in the field of engineering and applied physics. The study of thermal radiation effect is important in numerous applications such as condensed fuel combustion, solar energy collectors, heat exchangers, glass and ceramics manufacture, rocket-propulsion chambers and laser-processing of materials (Chen et al. 1993; Reddy and Kumar 2008; Nassab and Maramisaran 2009; Obidina and Kiseleva 1980; Saladino and Farmer 1993; Gedda et al. 2002).

The physics of the problem on radiation convection flows demands inclusion of the Schuster-Schwartzchild two flux model, the Milne-Eddington approximation and the Rosseland diffusion flux model (Siegel and Howell, 1972). Each flux model has its relative benefits and different regimes of validity. Davies (1995) studied the free and forced convection flow on a plate with thermal radiation by employing a heat- balance integral method. Chen et al. (1984) studied free gray absorbing - emitting, non-scattering convection boundary layer flow along an isothermal horizontal plate with thermal radiation flux by using the Rosseland diffusion model. Chamkha et al. (2004) have studied viscoelastic free convection boundary layer flow from a doubly inclined geometry, i.e., wedge, in porous media with the Rosseland diffusion flux model. Bestman (1995) studied asymptotic compressible flow along a long vertical hot plate in the presence of an externally applied magnetic field with strong radiative transfer and temperature dependent viscosity and thermal conductivity, using differential approximation for the radiative flux. Campo and Schuler (1988) investigated numerically the interaction of forced convection and thermal radiation heat transfer in laminar absorbing-emitting gray gas pipe flow by using the method of moments to approximate the radiative heat flux. Yih (1999) employed the Rosseland flux model to study the radiative effects on free convection boundary layer flow from an isothermal vertical cylinder in a porous medium (PM). Hossain et al. (2001) used the Rosseland diffusion radiation flux model to simulate the natural convection, variable viscosity heat transfer from a vertical plate with suction effects. An oscillating plate temperature effect on a flow past an infinite vertical porous late with constant suction and embedded in a PM was examined by Jaiswal and Soundalgekar (2001). Raptis and Perdikis (2003) discussed the thermal radiation of an optically thin gray gas. Muthucumaraswamy and Ganesan (2003) examined the radiation effects on flow past an impulsively started infinite vertical plate with variable temperature. Makinde (2005) employed a superposition technique and a Rosseland diffusion flux model to study the natural convection heat and mass transfer in a gray, absorbing-emitting fluid along a porous vertical translating plate. Kumar and Verma (2011) examined the thermal radiation and mass transfer effects on an MHD flow past a vertical oscillating plate with variable temperature and mass diffusion. An unsteady radiative flow past an oscillating semi-infinite vertical plate with uniform mass flux was presented by Muthucumaraswamy and Saravanan (2013). Muthucumaraswamy et al. (2014) studied the thermal radiation effects on an MHD flow past a vertical oscillating plate with chemical reaction of first order. Ghosh et al. (2015) investigated the transient MHD free convection flow of an optically thick gray gas past a moving vertical plate in

the presence of thermal radiation and mass diffusion. An MHD radiating heat/mass transport in a Darcian porous regime bounded by an oscillating vertical surface was presented by Ahmed et al. (2015).

The purpose of the present investigation is to deal with thermal radiation of an optically dense medium with temperature variation along an infinite oscillating vertical flat plate with a decisive importance to gravity-driven radiation-convection flow. The study of fluid flow problem by employing Rosseland diffusion flux model is significant for gray gas flows wherein the fluid is considered to be a gray, absorbing – emitting, but non- scattering medium. This problem is an improvement of Stoke's first and second problems to generate gravity driven radiation- convection flow, and has applications in space craft propulsion system, solar energy collectors and heat exchanges. As far as the authors are aware, this mathematical study has not been reported so far in the literature.

2. Formulation of the Problem and its Solution

We consider an unsteady flow of a viscous incompressible fluid occupying a semi-infinite region of space bounded by an infinite vertical flat plate (Figure 1) moving with uniform velocity u_0, which varies harmonically with time in the presence of natural convection and radiation. The fluid is considered to be a gray, absorbing-emitting, but non-scattering medium. Co-ordinate system is chosen in such a way that x'-axis is taken along the plate and y'-axis is normal to it.

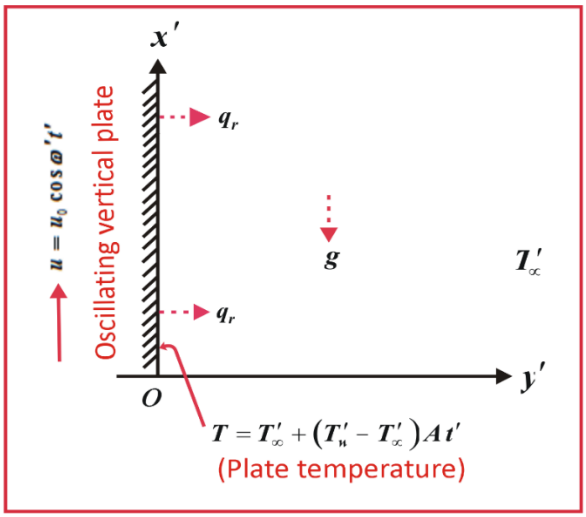

Figure 1: Geometry of the problem.

It is considered that all fluid properties are constant except the influence of density variation in the body force term. Initally, the plate and fluid are at same temperature in a stationary condition. At time $t' > 0$, the plate is given an impulsive motion in the vertical direction against the gravitional field with the constant velocity u_0, which varies harmonically with time and the plate temperature

is made to rise linearly with time. Since the plate is infinite along x'-direction, all physical quantites are functions of y' and t' only.

Under the Boussinesq approximation, the flow is governed by the following equation:

$$\frac{\partial u'}{\partial t'} = \nu \frac{\partial^2 u'}{\partial y'^2} + g\beta\left(T' - T'_\infty\right) \tag{1}$$

The energy equation becomes:

$$\frac{\partial T'}{\partial t'} = \frac{k}{\rho c_p}\frac{\partial^2 T'}{\partial y'^2} - \frac{1}{\rho c_p}\frac{\partial q_r}{\partial y'} \tag{2}$$

where $u', t', \nu, g, \beta, T', T'_\infty, k, c_p, \rho$ and q_r are respectively, the velocity component along the plate, the time, the kinematic coefficient of viscosity, the gravitational acceleration, the coefficient of thermal expansion, the temperature of the fluid, the temperature of the fluid far away from the plate, the thermal conductivity, the specific heat at constant pressure, the density of the fluid and the radiative heat-flux.

The boundary conditions are:

$$\begin{aligned} &u' = 0,\ T' = T'_\infty \ \text{ for all } y',\ t' \le 0 \\ &t' > 0 : u' = u_0 \cos\omega' t',\ T' = T'_\infty + \left(T'_w - T'_\infty\right) A t' \ \text{ at } y' = 0 \\ &u' \to 0,\ T' \to T'_\infty \ \text{ as } y' \to \infty \end{aligned} \tag{3}$$

where $A = u_0^2/\nu,\ T'_w$ is the temperature at the plate, u_0 is the velocity of the plate and ω' is the frequency of oscillations.

Introducing dimensionless quantities:

$$u = \frac{u'}{u_0},\quad y = \frac{y' u_0}{\nu},\quad t = \frac{t' u_0^2}{\nu},\quad \omega = \frac{\omega' \nu}{u_0^{\,2}}$$

$$T = \frac{T' - T'_\infty}{T'_w - T'_\infty},\quad \mathrm{Pr} = \frac{\nu}{a} = \frac{\rho \nu c_p}{k} \ \text{ and } \ \mathrm{Gr} = \frac{g\beta\nu\left(T'_w - T'_\infty\right)}{u_0^{\,3}} \ \text{ is the Grash of number} \tag{4}$$

The equation (1) together with the dimensionless quantities (4) transforms into:

$$\frac{\partial u}{\partial t} = \frac{\partial^2 u}{\partial y^2} + Gr\,T \tag{5}$$

In this problem, the large optical thickness is defined just as with molecular conductivity the transfer of radiant energy in a medium can be compared with diffusion transfer. Here the effect of interphoton collision is predominant. For large optical thickness (optically dense medium), a gray body radiation depends on the basis of diffusion concept of radiation heat transfer. The radiation flux vector can be found from Isachenko et al. (1980) and its formula is derived on the basis of the diffusion concept of radiation heat transfer in the following way:

$$q_r = -\frac{4\sigma}{3k^*}\frac{\partial T'^4}{\partial y'} \tag{6}$$

where σ and k^* are respectively, the Stefan-Boltzman constant and the spectrul mean absorption coefficient of the medium.

It is assumed that the temperature differences within the flow are sufficiently small such that T'^4 may be regarded as a linear function of temperature. It can be established by expanding T'^4 i.e., a Taylor series about T'_∞ and neglecting higher order term. Therefore T'^4 can be expressed in the following way

$$T'^4 = 4T'^3_\infty T' - 3T'^4_\infty \tag{7}$$

Using (6) and (7), equation (2) takes the form

$$\frac{\partial T'}{\partial t'} = \frac{k}{\rho c_p}\frac{\partial^2 T'}{\partial y'^2} + \frac{16\sigma T'^3_\infty}{3k^*}\frac{1}{\rho c_p}\frac{\partial^2 T'}{\partial y'^2} \tag{8}$$

Using dimensionless quantities (4) , the equation (8) can be written in a dimensionless form

$$\left(1+k_1\right)\frac{\partial^2 T}{\partial y^2} - \Pr\frac{\partial T}{\partial t} = 0 \tag{9}$$

where $k_1 = \dfrac{16\sigma T'^3_\infty}{3k^* k}$ is the radiation parameter.

The dimensionless boundary conditions turn into

$$\begin{aligned} &u = 0,\ T = 0 \ \text{ for all } \ y,\ t \le 0 \\ &t > 0:\ u = \cos\omega t,\ T = t \ \text{ at } \ y = 0 \\ &u \to 0,\ T \to 0 \ \text{ at } \ y \to \infty \end{aligned} \tag{10}$$

Applying Laplace transform of (5) and (9) in the following

$$su^* = \frac{\partial^2 u^*}{\partial y^2} + \mathrm{Gr}T^* \tag{11}$$

$$\left(1+k_1\right)\frac{\partial^2 T^*}{\partial y^2} - \Pr s T^* = 0 \tag{12}$$

The corresponding boundary conditions become

$$\begin{aligned} &u^* = 0,\ \ T^* = 0 \ \text{ for all } \ y,\ \frac{1}{s^2} \le 0 \\ &\frac{1}{s^2} > 0:\ u^* = \frac{s}{s^2+\omega^2},\ T^* = \frac{1}{s^2} \ \text{ at } \ y = 0 \\ &u^* \to 0,\ T^* \to 0 \ \text{ at } \ y \to \infty \end{aligned} \tag{13}$$

$$\text{Here,} \quad u^* = \frac{s}{s^2+\omega^2} = \frac{1}{2}\left[\frac{1}{s+i\omega} + \frac{1}{s-i\omega}\right] \tag{14}$$

By applying temperature boundary conditions given by (13), equation (12) becomes

$$T^* = \frac{1}{s^2} e^{-\sqrt{\frac{\Pr s}{1+k_1}}\, y} \tag{15}$$

Using (15), equation (11) becomes

$$s u^* = \frac{\partial^2 u^*}{\partial y^2} + \frac{\mathrm{Gr}}{s^2} e^{-\sqrt{\frac{\Pr s}{1+k_1}}\, y} \tag{16}$$

By applying Laplace inversion method, the equation (14) gives

$$\mathrm{L}^{-1}\left\{\frac{1}{s+i\omega}\right\} = e^{-i\omega t}, \quad \mathrm{L}^{-1}\left\{\frac{1}{s-i\omega}\right\} = e^{i\omega t}, \quad \mathrm{L}^{-1}\left\{e^{-\sqrt{s}y}\right\} = \frac{y}{2\sqrt{\pi t^3}} e^{-\frac{y^2}{4t}} \tag{17}$$

Using Convolution theorem with reference to Laplace Inversion method together with the boundary condition (13) subject to (17), the solution of velocity and temperature distribution with reference to (16) and (15) such as

$$u(y,t) = \frac{1}{4}\left[e^{\left(y\sqrt{-i\omega}-i\omega t\right)}\mathrm{erfc}\left(\frac{y}{2\sqrt{t}} + \sqrt{-i\omega t}\right) + e^{-\left(y\sqrt{-i\omega}+i\omega t\right)}\mathrm{erfc}\left(\frac{y}{2\sqrt{t}} - \sqrt{-i\omega t}\right)\right.$$

$$\left. + e^{\left(y\sqrt{i\omega}+i\omega t\right)}\mathrm{erfc}\left(\frac{y}{2\sqrt{t}} + \sqrt{i\omega t}\right) + e^{-\left(y\sqrt{i\omega}-i\omega t\right)}\mathrm{erfc}\left(\frac{y}{2\sqrt{t}} - \sqrt{i\omega t}\right)\right]$$

$$+ \frac{\mathrm{Gr}}{\alpha-1}\left[\left\{\frac{1}{2}\left(t^2 + y^2 t\right) + \frac{y^4}{24}\right\}\mathrm{erfc}\left(\frac{y}{2\sqrt{t}}\right) - y\sqrt{\frac{t}{\pi}}\left(\frac{5}{6}t + \frac{y^2}{12}\right)e^{-\frac{y^2}{4t}}\right]$$

$$- \frac{\mathrm{Gr}}{\alpha-1}\left[\left\{\frac{1}{2}\left(t^2 + \alpha y^2 t\right) + \frac{\alpha^2}{24}y^4\right\}\mathrm{erfc}\left(\frac{y\sqrt{\alpha}}{2\sqrt{t}}\right) - y\sqrt{\alpha}\sqrt{\frac{t}{\pi}}\left(\frac{5}{6}t + \frac{y^2\alpha}{12}\right)e^{-\frac{y^2\alpha}{4t}}\right] \tag{18}$$

where ω and ωt are, respectively, the dimensionless frequency of oscillations and phase angle and

$$T(y,t) = \left(t + \frac{y^2}{2}\alpha\right)\mathrm{erfc}\left(\frac{y}{2}\sqrt{\frac{\alpha}{t}}\right) - y\sqrt{\alpha}\sqrt{\frac{t}{\pi}}\, e^{-\frac{y^2\alpha}{4t}}, \tag{19}$$

where $\alpha = \dfrac{\Pr}{1+k_1}$

Particular case of interest:

Non–oscillatory case by putting $\omega = 0$ and $\omega t = 0$.The dimensionless boundary conditions (10) turns into

$$\begin{aligned} &u=0,\ T=0 \quad \text{for all} \quad y,\ t\le 0 \\ &t>0: u=1,\ T=t \ \text{ at } y=0 \\ &u\to 0,\ \ T\to 0 \ \text{ as } \ y\to\infty \end{aligned} \tag{20}$$

By applying Laplace transform subject to equations (11) and (12) together with the boundary condition (20) the velocity and temperature distribution can be obtained by the help of Laplace Inversion method such as

$$\begin{aligned} u(y,t) &= \operatorname{erfc}\left(\frac{y}{2\sqrt{t}}\right)+\frac{\mathrm{Gr}}{\alpha-1}\left[\left\{\frac{1}{2}\left(t^2+y^2t\right)+\frac{y^4}{24}\right\}\operatorname{erfc}\left(\frac{y}{2\sqrt{t}}\right)-y\sqrt{\frac{t}{\pi}}\left(\frac{5}{6}t+\frac{y^2}{12}\right)e^{-\frac{y^2}{4t}}\right] \\ &-\frac{\mathrm{Gr}}{\alpha-1}\left[\left\{\frac{1}{2}\left(t^2+\alpha y^2t\right)+\frac{\alpha^2y^4}{24}\right\}\operatorname{erfc}\left(\frac{y\sqrt{\alpha}}{2\sqrt{t}}\right)-y\sqrt{\alpha}\sqrt{\frac{t}{\pi}}\left(\frac{5}{6}t+\frac{y^2\alpha}{12}\right)e^{-\frac{y^2\alpha}{4t}}\right] \\ T(y,t) &= \left(t+\frac{y^2}{2}\alpha\right)\operatorname{erfc}\left(\frac{y}{2}\sqrt{\frac{\alpha}{t}}\right)-y\sqrt{\alpha}\sqrt{\frac{t}{\pi}}\,e^{-\frac{y^2\alpha}{4t}} \end{aligned} \tag{21}$$

Shear stress at the plate $y=0$ for $\omega=0$ and $\omega t=0$

$$\tau_x=\left.\frac{du}{dy}\right|_{y=0}=-\frac{1}{\sqrt{\pi t}}-\frac{4}{3}\frac{\mathrm{Gr}}{\alpha-1}t\sqrt{\frac{t}{\pi}}+\frac{1}{2}t\sqrt{\frac{t}{\pi}}\frac{\mathrm{Gr}}{\alpha-1}\left(1-\frac{5}{3}\sqrt{\alpha}\right) \tag{22}$$

In the absence of Grashof number $(\mathrm{Gr}=0)$ the velocity distribution $u(y,t)$ given by (21) takes place

$$u(y,t)=\operatorname{erfc}\left(\frac{y}{2\sqrt{t}}\right) \tag{23}$$

Equation (23) gives the velocity of Stoke's first problem where

$$u(y,t)=\operatorname{erfc}\left(\frac{y}{2\sqrt{t}}\right)=1-\operatorname{erf}\left(\frac{y}{2\sqrt{t}}\right)$$

The temperature distribution (19) gives the Nusselt number Nu at the plate

$$Nu=-\left.\frac{dT}{dy}\right|_{y=0}=2\sqrt{\frac{t}{\pi}}\sqrt{\frac{\mathrm{Pr}}{1+k_1}} \tag{24}$$

3. Results and Discussion

Numerical solution have been computed from the analytical solutions given by (18) and (19). The regime is controlled by six physical parameters namely, radiation parameter (k_1), Grashof number (Gr), Prandtl number (Pr), frequency parameter (ω), phase angle (ωt) and time (t). The flow regime is characterised by its fluid velocity and temperature distribution which are depicted graphically in Figures 2-12 for various values of k_1, Gr, Pr, ωt and t. In all cases we have considered air $(\mathrm{Pr}=0.72)$. Fig 2. illustrates the influence of the Rosseland radiation -conduction parameter (k_1)

on velocity profiles for $(\mathrm{Pr}=0.72)$ i.e. $\mathrm{Pr}<1$, so that heat diffuses faster than momentum in the regime. With an increase in k_1 i.e. stronger thermal radiation flux, there is a slight increment in the velocity in close proximity to the plate surface. Closer to the plate there is a linear decay to converge the velocity profiles for any k_1. It is interesting to note that back flow occurs near the plate surface for $k_1>3$. This will happen in the case of an oscillating flow on increasing k_1 to become a reverse flow near the plate surface. In Figures 3 and 4, the influence of Grashof number (Gr) on velocity field leads to increase the flow behavior for small as well as large values of Gr. The thermal Grashof number signifies the relative effect of the thermal buoyancy (due to density differences) force to the viscous hydrodynamic force in the boundary layer flow. The positive values of Gr correspond to cooling of the plate by natural convection. It is observed that the transient velocity accelerates due to enhancement in the thermal buoyancy force, that is, free convection effects. As the buoyancy effects become relatively large due to increasing value of Gr, the fluid velocity increases, reaching its peak value near the plate surface and then decreases monotonically to the zero-free stream value satisfying the far field condition. For the case of higher buoyancy it may be noted from Figure 4 that there is no flow reversal on velocity field and the maximum peak of the profile occurs at the plate $y=0$ while the peak of the profile decreases steadily near the plate surface. In the case of an oscillating plate, the flow velocity is charactarised by the higher buoyancy to increase the fluid velocity with an increase in Gr. We note that both Figures 3 and 4 correspond to short time elapse after the impulsive motion onset i.e. $\mathrm{t}=0.2$. It is evident from Figure 5 that the fluid velocity decreases with an increase of phase angle (ωt). This situation reavels that the time oriented angular frequency of oscillation (ωt) reduces the flow velocity on increasing ωt with reference to impulsive onset of the motion. There arises a phase lag on molecular diffusion region with interphoton collision. It is noticed from Figure 6 that in the absence of Grashof number, the oscillating field of flow approaches Stoke's second problem which leads to decrease the fluid velocity with an increase in phase angle (ωt). Figure 7 demonstrates that with the increase in Prandtl number (Pr) the fluid velocity decreases near the plate surface. Physically, this is possible because fluids with high Prandtl numbers have high viscosity and hence move slowly that is smaller values of Pr are equivalent to increasing the thermal conductivity, and therefore heat is able to diffuse away from the heated surface more rapidly than of higher values of Pr. These results agree with the earlier results of Ahmed et al. (2015). It is interesting to note that there arise flow reversal near the plate surface for $\mathrm{Pr}>1$. Since the Prandtl number corresponds to diffusion concept of the flow medium the flow velocity is characterised by the oscillating plate to imped back flow on the plate surface with reference to diffusivity of the flow medium. Figure 8 shows that for buoyancy added flow $(\mathrm{Gr}>0)$ the velocity increases with increase in time (t). The maximum peak of the velocity profiles occurs adjacent to the plate whereas the peak of the profiles quickly decreases on the plate surface. Since the plate oscillates harmonically with time, the velocity profiles are skewed near the plate surface. The skewness is characterised by the impulsive movement of the plate with time variation at the

plate. It is observed from Figure 9 that in the absence of oscillation $(\omega = 0 \text{ and } \omega t = 0)$ and $(\mathrm{Gr} = 0)$, this represents Stoke's flow with reference to the velocity distribution $u(y,t) = \mathrm{erfc}\left(\frac{y}{2\sqrt{t}}\right) = 1 - \mathrm{erf}\left(\frac{y}{2\sqrt{t}}\right)$. This situation reveals that the velocity increases with increase in time t which corresponds to Stoke's first problem in fluid dynamics. Figure 10 shows that the temperature field (T) increases with an increase in radiation parameter (k_1). Larger (k_1) values correspond to an increased dominance of thermal radiation over conduction. As such thermal radiation supplements the thermal diffusion and increases the overall thermal diffusivity of the regime since the local radiant diffusion flux model adds radiation conductivity to the conventional thermal conductivity. As a result, the fluid temperature and velocity in the fluid regime of flow are increased. Figure 11 demontrates that with the increase in Prandtl number (Pr) the temperature field (T) decreases near the plate. This is true since; in general, fluid with low Prandtl number has higher thermal conductivity. The higher thermal conductivity means fluid has affinity for heat and so low Prandtl fluid attains comparatively higher temperature. The effect of Prandtl number plays a significant role on diffusion concept of flow medium. If Prandtl number is greater than one ($\mathrm{Pr} > 1$) the diffisivity of the flow medium tends to ionization of the flow. In a highly ionized fluid $\mathrm{Pr} > 1$, the effect of Prandtl number ($\mathrm{Pr} = 0.72$) from ionized state to water. Figure 12 reveals that with an increase in t, there is a strong acceleration in the flow. It is stated that the temperature field (T) increases with an increase in time (t). Thus, time variation at the plate gives rise to increase in temperature with an increase in time (t).

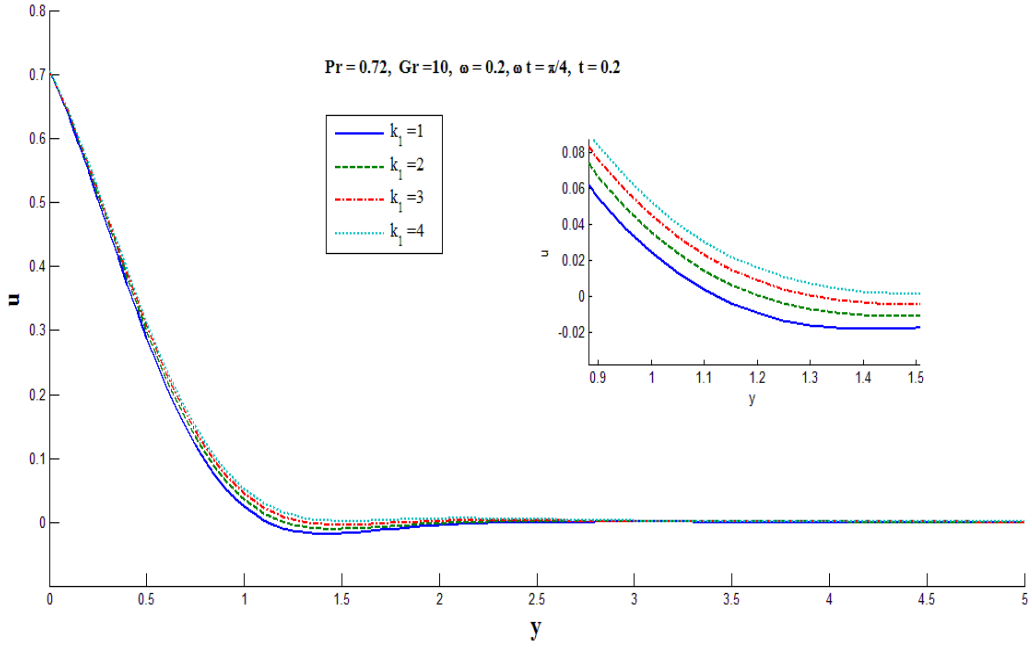

Figure 2: Velocity profiles for increasing $\mathbf{k_1}$.

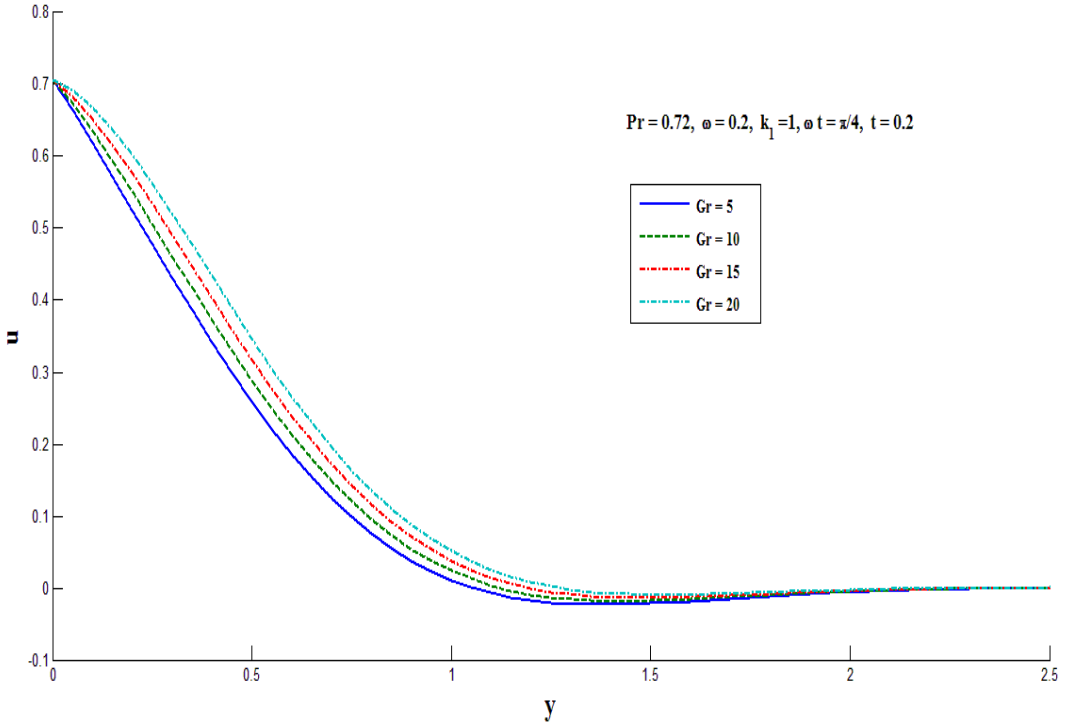

Figure 3: Velocity profiles for small Grashof number **Gr** .

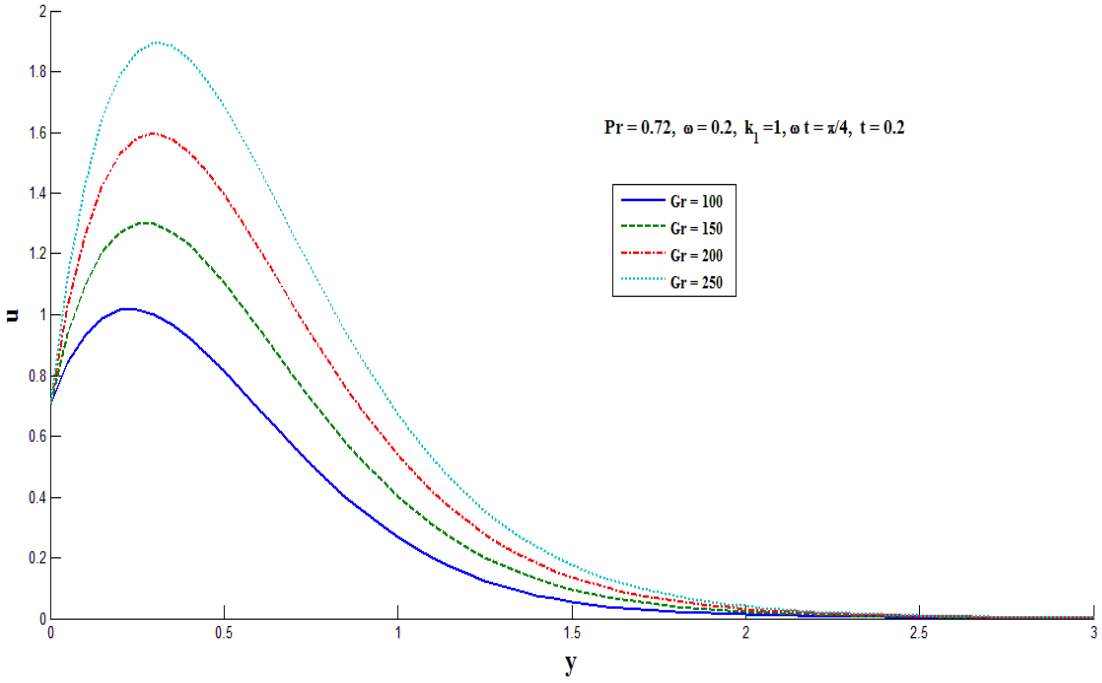

Figure 4: Velocity profiles for large Grashof number **Gr** .

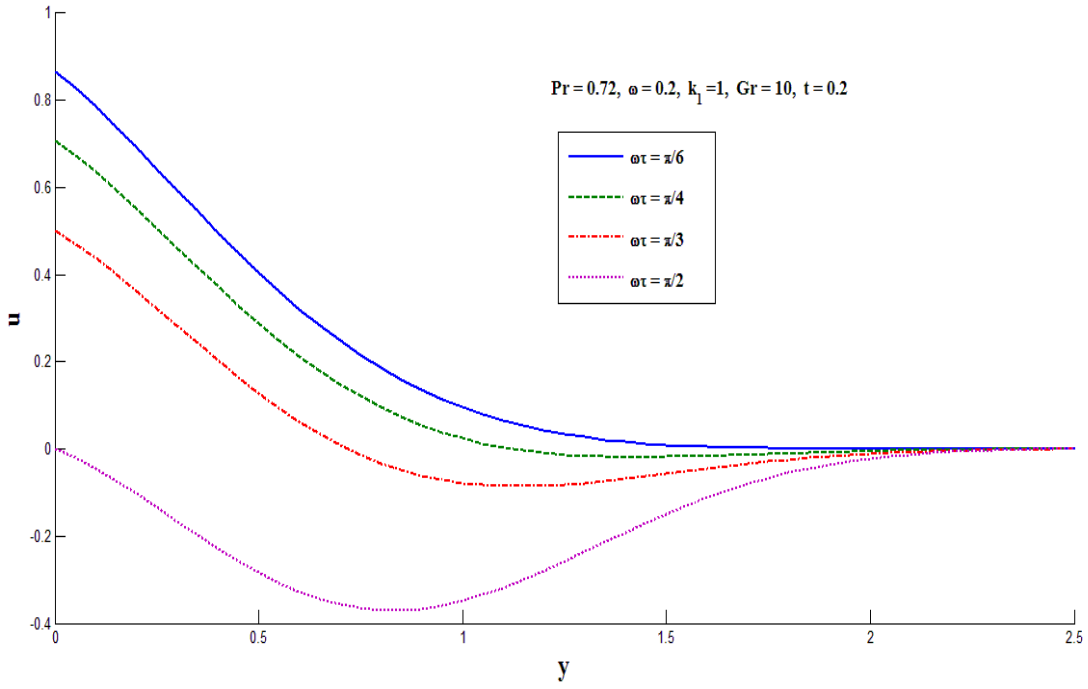

Figure 5: Velocity profiles for increasing ωt

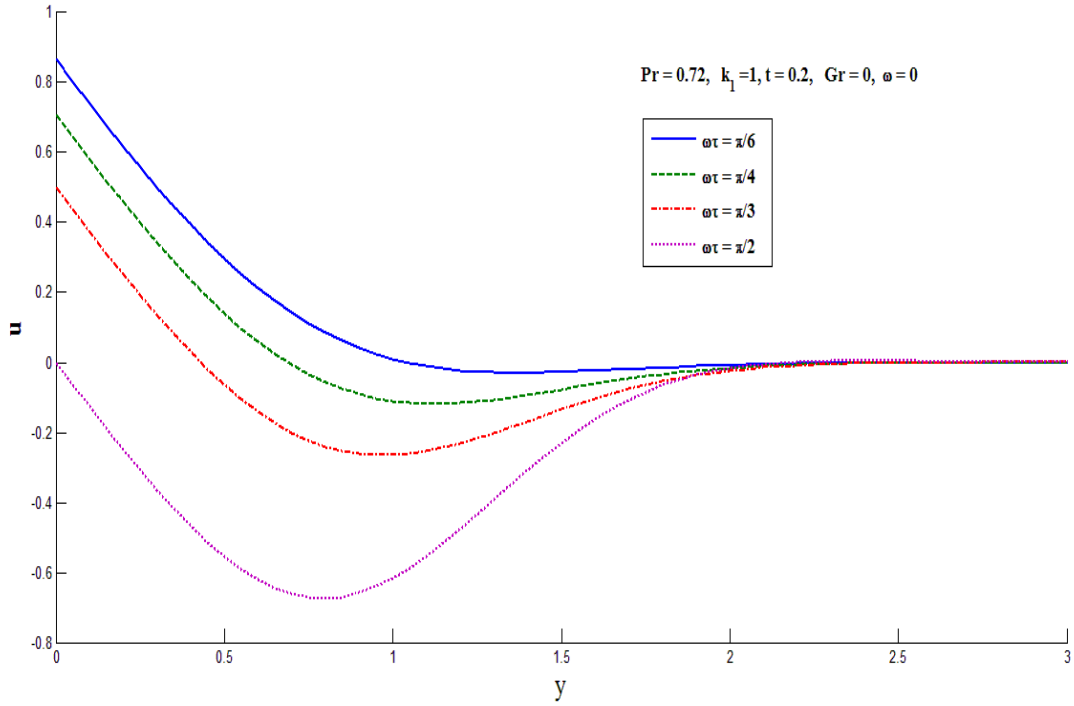

Figure 6: Velocity profiles for increasing ωt (Stoke's Problem)

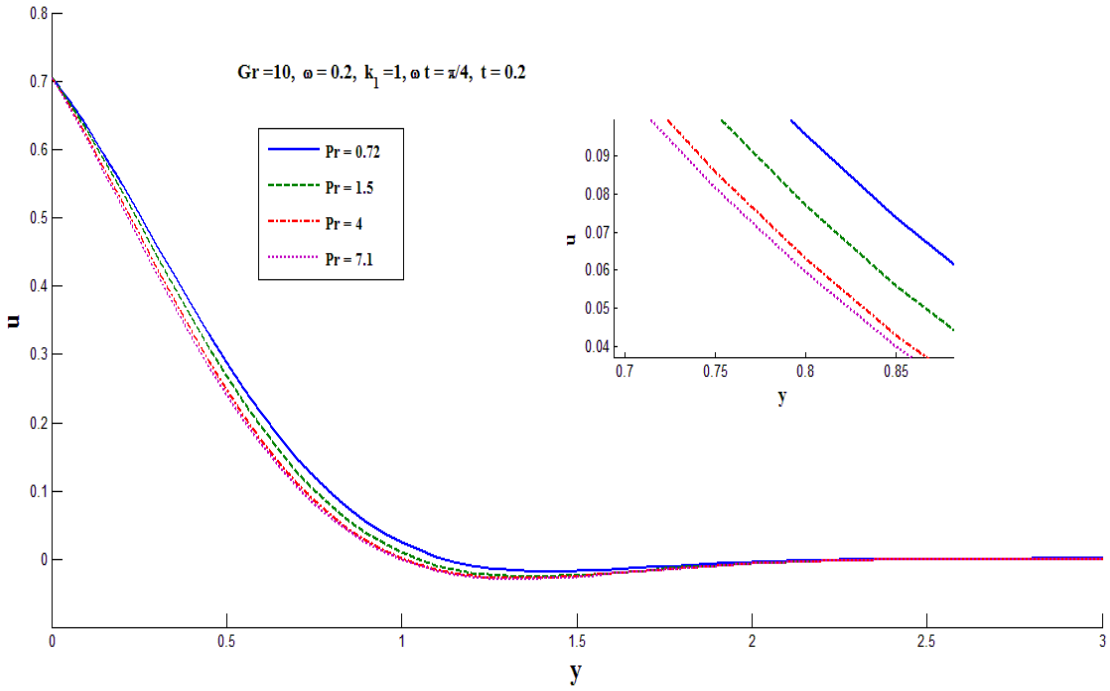

Figure 7: Velocity profiles for increasing **Pr**

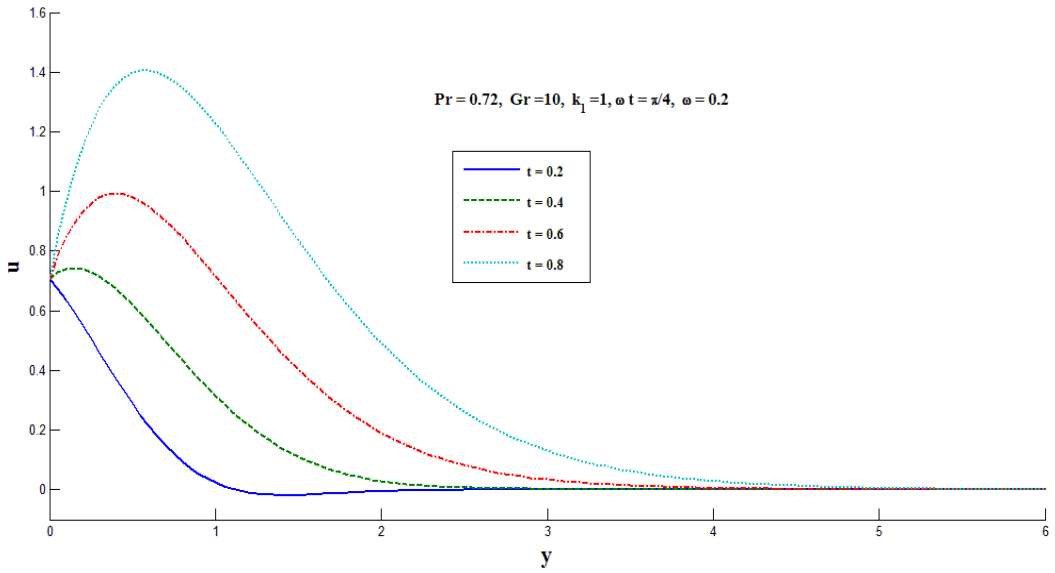

Figure 8: Velocity profiles for increasing time ***t***

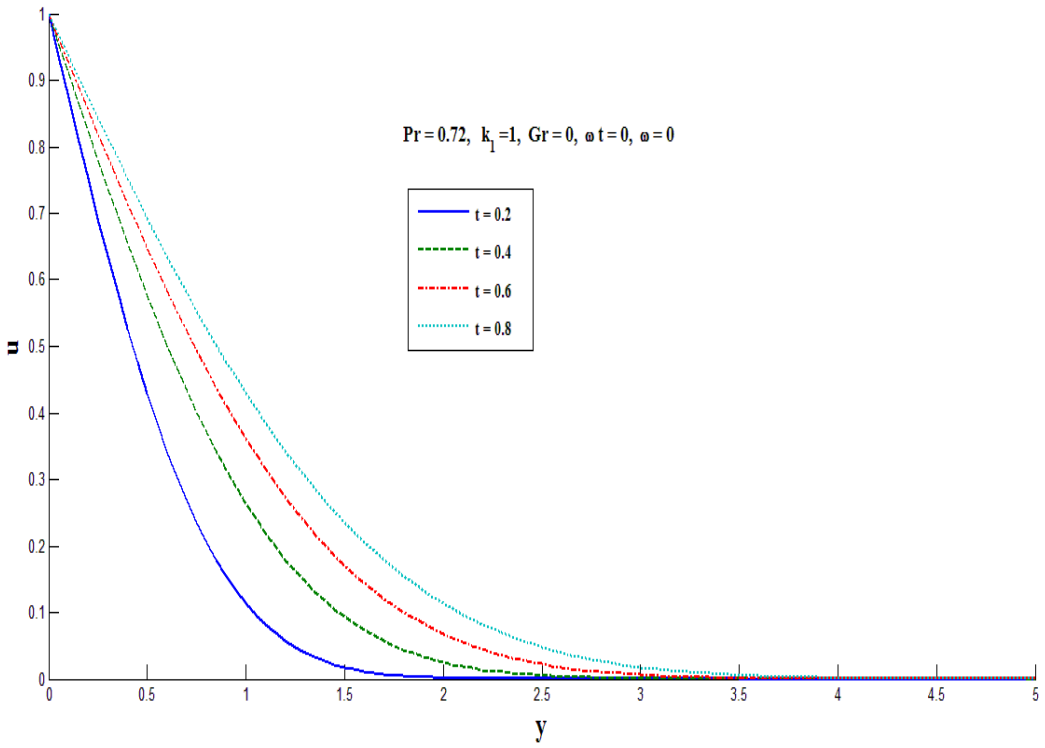

Figure 9: Velocity profiles for increasing time t (Stoke's Problem)

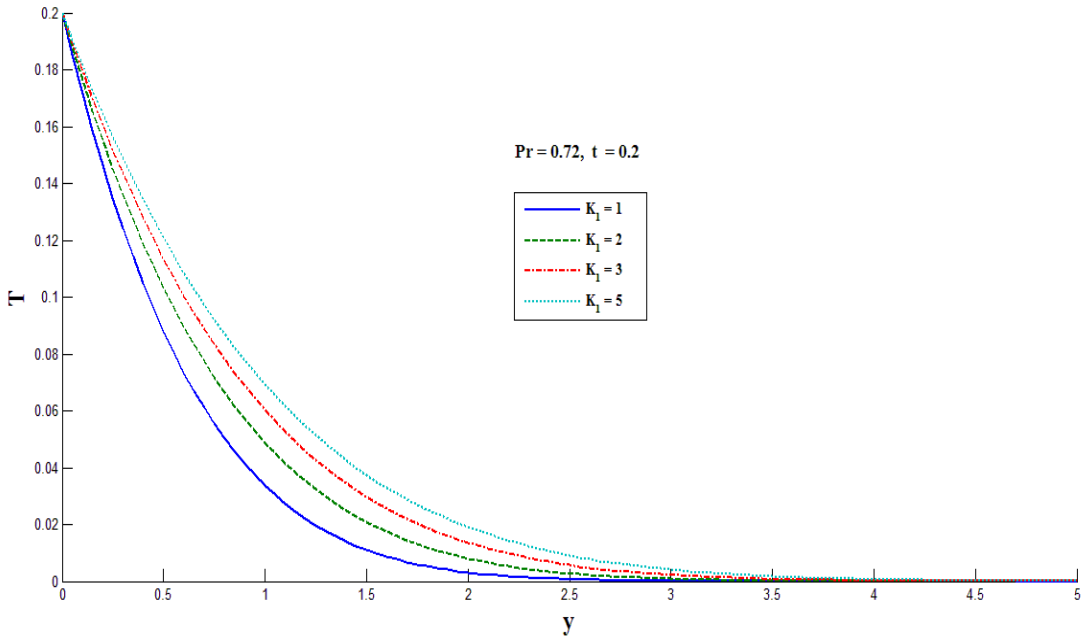

Figure 10: Temperature profiles for increasing k_1.

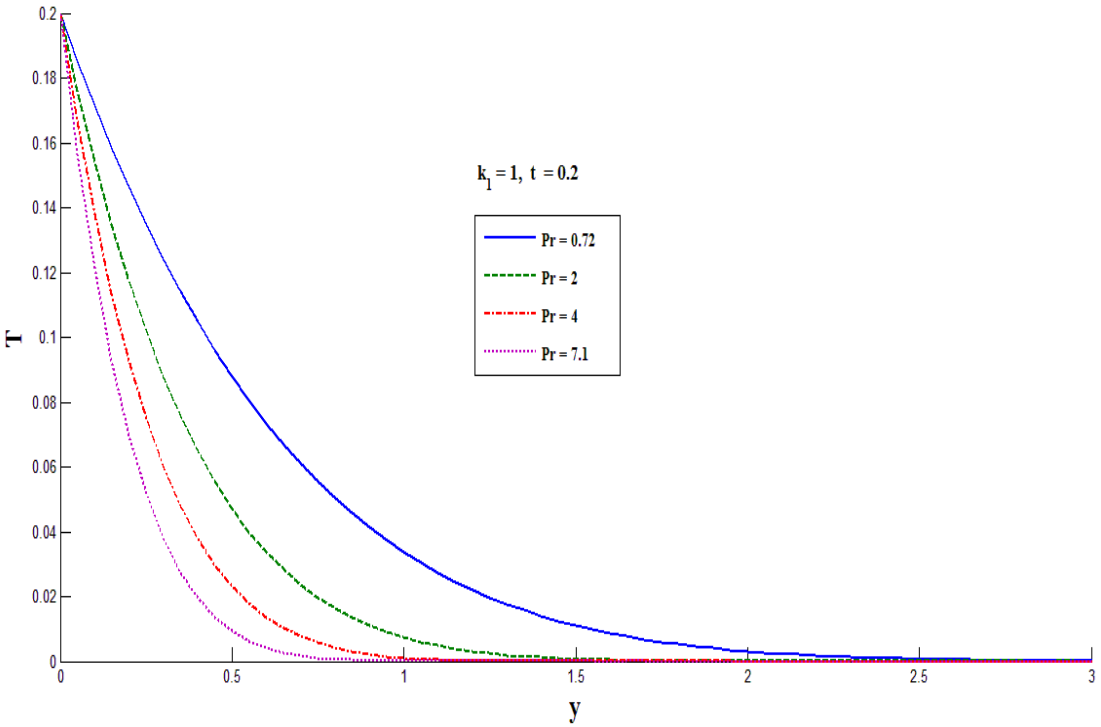

Figure 11: Temperature profiles for increasing **Pr** .

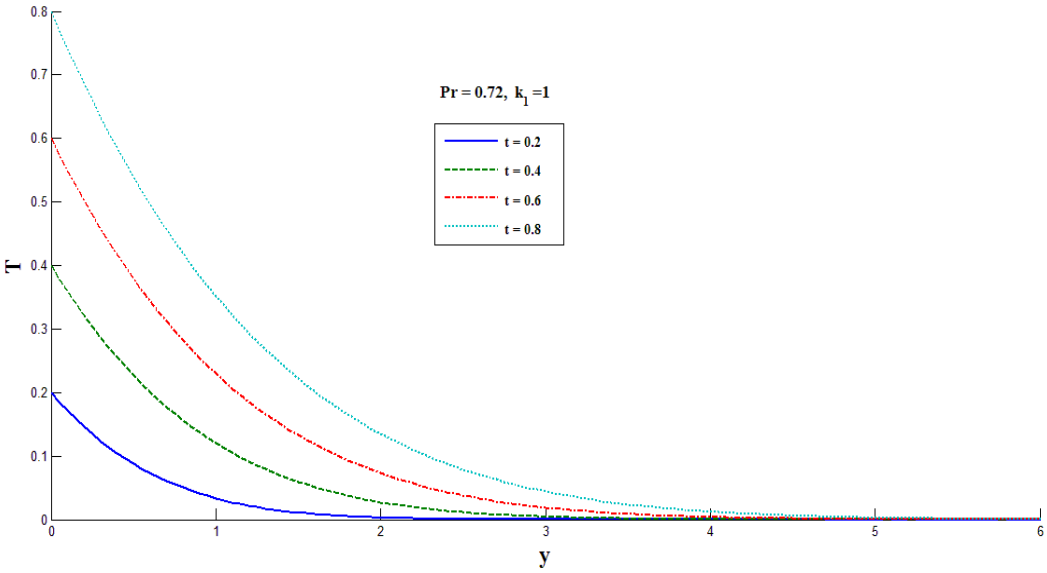

Figure 12: Temperature profiles for increasing time t

Frictional shear stress at the plate ($y = 0$):

Frictional shearing stress at the plate can be obtained from $\left.\frac{du}{dy}\right|_{y=0} = 0$ with reference to the solution $u(y,t)$ of (18)

$$\tau_x = \left.\frac{du}{dy}\right|_{y=0}$$

$$= \frac{1}{4}\left[-\frac{2}{\sqrt{\pi t}} + \sqrt{-i\omega}\, e^{-i\omega t}\left\{\operatorname{erfc}\left(\sqrt{-i\omega t}\right) - \operatorname{erfc}\left(-\sqrt{-i\omega t}\right)\right\}\right.$$

$$\left. -\frac{2}{\sqrt{\pi t}} + \sqrt{i\,\omega} e^{i\omega t}\left\{\operatorname{erfc}\left(\sqrt{i\omega t}\right) - \operatorname{erfc}\left(-\sqrt{i\,\omega t}\right)\right\}\right] + \frac{5}{6}\frac{\mathrm{Gr}}{\alpha - 1}\; t\sqrt{\frac{t}{\pi}}\left(\sqrt{\alpha} - 1\right) \qquad (25)$$

Critical Grashof Number:

Critical Grashof Number can be obtained by putting $\left.\frac{du}{dy}\right|_{y=0} = 0$ in equation (25)

$$\mathrm{Gr}_{\mathrm{crit}} = \frac{1}{A\sqrt{\pi t}} - \frac{1}{4A}\left[\sqrt{-i\omega}\; e^{-i\,\omega t}\left\{\operatorname{erfc}\left(\sqrt{-i\omega\, t}\right) - \operatorname{erfc}\left(-\sqrt{-i\omega t}\right)\right\}\right.$$

$$\left. +\sqrt{i\omega}\; e^{i\omega t}\left\{\operatorname{erfc}\left(\sqrt{i\omega t}\right) - \operatorname{erfc}\left(-\sqrt{i\omega t}\right)\right\}\right] \qquad (26)$$

where $A = \frac{5}{6}\frac{1}{\alpha - 1} t\sqrt{\frac{t}{\pi}}\left(\sqrt{\alpha} - 1\right)$

Nusselt number Nu at the plate becomes

$$2\sqrt{\frac{\alpha t}{\pi}} \qquad (27)$$

Numerical results of shear stress and critical Grashof number are presented in Tables 1 to 5. Table 1 shows that the frictional shear stress at the plate increases with an increase in either k_1 or t. There exists separation at the plate for $t > 0.2$, and also frictional drag increases to impede thermal diffusion at the plate surface. Table 2 demonstrates that the frictional shear stress decreases in magnitude with increase in either Gr or k_1. This implies the situation of drag-reducing effect to produce stronger thermal diffusion at the plate surface. It is noticed from Table 3 that the frictional shear stress increases with an increase in either ω_t or t. It is interesting to note that there exists separation when $t > 0.4$. Since phase angle rotates about the time variation at the plate the frictional drag is increased to show the influence of thermal radiation at the plate surface. It is evident from Table 4 that there arises a destabilizing influence on the flow field on increasing either k_1 or t. Table 5 indicates that Gr_{crit} decreases with increase in either ω_t or t to show the influence of destabilizing effect on the flow field. It is noticed from Tables 4 and 5 that no flow reversal occurs at the plate surface.

Table 1: Shear stress at the plate τ_x for $\mathrm{Pr} = 0.72,\ \mathrm{Gr} = 10,\ \omega = 0.2$ and $\omega t = \frac{\pi}{4}$

t/k_1	1.0	2.0	3.0	4.0	5.0
0.2	– 0.78045	– 0.76103	– 0.76802	– 0.73844	– 0.73095
0.4	0.06960	0.12454	0.16132	0.18844	0.20961
0.6	0.85560	0.95652	1.02411	1.07392	1.11282
0.8	1.69011	1.84549	1.94954	2.02623	2.08612
1.0	2.59257	2.80973	2.95515	3.06233	3.14602

Table 2: Shear stress at the plate τ_x for $\mathrm{Pr} = 0.72,\ \omega = 0.2,\ \omega t = \frac{\pi}{4}$ and $t = 0.2$

Gr/k_1	5.0	10.0	15.0	20.0	25.0
1.0	– 0.91187	– 0.78045	– 0.64905	– 0.51763	– 0.38621
2.0	– 0.90216	– 0.76103	– 0.61991	– 0.47878	– 0.33766
3.0	– 0.89565	– 0.74802	– 0.60040	– 0.45277	– 0.30514
4.0	– 0.89086	– 0.73844	– 0.58602	– 0.43360	– 0.28117
5.0	– 0.88712	– 0.73095	– 0.57479	– 0.41862	– 0.26246

Table 3: Shear stress at the plate τ_x for $\mathrm{Pr} = 0.72,\ \omega = 0.2,\ \mathrm{Gr} = 10$ and $k_1 = 1$

$t/\omega t$	0.0	$\pi/6$	$\pi/4$	$\pi/3$	$\pi/2$
0.2	– 0.99874	– 0.78045	– 0.78045	– 0.68115	– 0.50544
0.4	– 0.14867	– 0.76103	0.06960	0.16890	0.34462
0.6	0.63731	0.76096	0.85560	0.95490	1.13062
0.8	1.47182	1.59547	1.69011	1.78941	1.96512
1.0	2.37429	2.49794	2.59257	2.69188	2.86759

Table 4: Critical Grashof number $\mathrm{Gr}_{\mathrm{crit}}$ for $\mathrm{Pr} = 0.72,\ \omega = 0.2$ and $\omega t = \frac{\pi}{4}$

t/k_1	1.0	2.0	3.0	4.0	5.0
0.2	39.69485	36.96329	35.33497	34.22374	33.40347
0.4	9.06368	8.43998	8.06817	7.81444	7.62715
0.6	3.73500	3.47798	3.32477	3.22021	3.14303
0.8	1.96185	1.82685	1.74637	1.69145	1.65091
1.0	1.17716	1.09615	1.04787	1.01491	0.99059

Table 5: Critical Grashof number Gr_{crit} for $Pr = 0.72$, $k_1 = 1.0$ and $\omega = 0.2$

$t/\omega t$	0^0	$\pi/6$	$\pi/4$	$\pi/3$	$\pi/2$
0.2	48.00001	43.29557	39.69485	35.91665	29.23097
0.4	12.00000	10.33673	9.06368	7.72789	5.36414
0.6	5.33333	4.42796	3.73500	3.00789	1.72123
0.8	3.00000	2.41194	1.96185	1.48958	0.65387
1.0	1.92000	1.49922	1.17716	0.83923	0.24124

4. Conclusion

A mathematical study has been conducted with reference to the transient approach on laminar gray gas flow of an optically thick fluid past an oscillating vertical flat plate in the presence of thermal radiation. The governing equations have been solved by using Laplace Transform method. Based on the graphical presentations, the conclusions can be summarized as follows:

- The velocity profiles are influenced by the Rosseland radiation – conduction parameter.
- The fluid velocity greatly increases for increasing values of Grashof number.
- The fluid velocity is accelerated when time progresses.
- The fluid temperature rises due to increasing radiation parameter or time while it falls for increasing values of Prandtl number.
- The frictional shear stress at the plate is reduced in magnitude with increase in Grashof number or radiation parameter while it is enhanced for increasing values of phase angle.
- The critical Grashof number increases for increasing values of phase angle or time whereas it decreases for increasing values of radiation parameter.

References

Ahmed S, Batin A, Chamkha AJ. (2015). Numerical/Laplace transform analysis for MHD radiating heat/mass transport in a Darcian porous regime bounded by an oscillating vertical surface, Alexandria Eng. J. 54: 45 - 54.

Bestman AR. (1985). Compressibility effect on laminar convection to a radiating gas past a vertical plate, Z. Angew, Math. Phys. 36 (5): 767-774.

Chamkha AJ, Takhar HS, Beg OA. (2004). Radiative free convective non-Newtonian fluid flow past a wedge embedded in a porous medium, Int. J. Fluid Mech. Res. 31 (2): 1-15.

Chen S L, Ma H K, Chen DY. (1993). Radiation blockage by the interaction of thermal radiation with conduction and convection in the conbustion of the condensed fuel, Int. Commun. Heat and Mass Transfer. 20: 145-157.

Chen TS, Ali AA, Armaly BF. (1984). Natural convection radiation interaction in boundary layer flow over horizontal surface, AIAA J. 22 (12): 1797-1803.

Compo A, Schuler C. (1988). Thermal radiation and laminar forced convection in a gas pipe flow, Heat Mass Transfer 22 (5): 251-257.

Davies TW. (1995). The cooling of a plate by combined thermal radiation and convection, Int. Commun. Heat Mass Transfer. 12: 405-415.

Gedda H, Powell J, Wahlstrom G, Li WB, Engstrom H, Magnusson C. (2002) . Energy redistribution during laser cladding, J. Laser Appli. 14: 78-82.

Ghosh SK, Das S, Jana RN. (2015), Transient MHD free convection flow of an optically thick gray gas past a moving vertical plate in the presence of thermal radiation and mass diffusion, J. Appl. Fluid Mech. 8: 65-73.

Hossain MA, Khanafer K, Vafai K. (2001). The effect of radiation on free convection flow of fluid with variable viscosity from a porous vertical plate, Int. J. Thermal Sci. 40: 115-124.
Isachenko VP, Osipova VA. (1980). Sukomel AS, Heat Transfer, Mir Publishers, Moscow, USSR.

Jaiswal BS, Soundalgekar VM. (2001). Oscillating plate temperature effects on a flow past an infinite vertical porous late with constant suction and embedded in a porous medium, Heat and Mass Transfer. 37: 125-131.

Kumar AGV, Verma SVK. (2011). Thermal radiation and mass transfer effects on MHD flow past a vertical oscillating plate with variable temperature effects variable mass diffusion, Int. J. Eng. 3: 493–499.

Makinde OD. (2005). Free convection flow with thermal radiation and mass transfer past a moving vertical porous plate, Int. Commun. Heat and Mass Transfer. 32: 1411-1419.
Muthucumaraswamy R, Ganesan P. (2003). Radiation effects on flow past an impulsively started infinite vertical plate with variable temperature, Int. J. Appl. Mech. Eng. 8(1): 125-129.

Muthucumaraswamy R, Nagarajan G, Subramanian VSA. (2014). Thermal radiation and MHD effects on flow past an vertical oscillating plate with chemical reaction of first order, Acta Technica Corvininesis - Bulletin of Eng. 7(3): 97.

Muthucumaraswamy R, Saravanan B. (2013). Numerical solution of unsteady radiative flow past an oscillating semi-infinite vertical plate with uniform mass flux, Comp. Methods in Sci. Tech. 19(1): 1-9.

Nassab SAG, Maramisaran M. (2009). Transient numerical analysis of a multi layered porous heat exchanger including gas radiation effects, Int. J. Thermal Sci. 48: 1586-1595.

Obidina SP, Kiseleva MN. (1980). Production of glass with high radiation absorption in the range 0.9–1.2, Glass and Ceramics. 37: 376-378.

Raptis A, Perdikis C. (2003). Thermal radiation of an optically thin gray gas, Int. J. Appl. Mech. Eng. 8(1): 131-134.

Reddy KS, Kumar N S. (2008).Combined laminar natural convection and surface radiation heat transfer in a modified cavity receiver of solar parabolic dish, Int. J. Thermal Sci. 47: 1647-1657.

Saladino AJ, Farmer RC. (1993). Radiation/Convection coupling in rocket motor and plume analysis, Final report, SECA Inc., Huntsville, Alabama, USA.

Siegel R, Howell JR. (1972). Thermal radiation Hear Transfer, Student edition, Mac Graw Hill, 1972.

Yih KA. (1999). Radiation effect on natural convection over a vertical cylinder embedded in a porous media, Int. Commum. Heat and Mass Transfer. 26: 259-267.